Parolai, S., Orunbaev, S., Bindi, D., Strollo, A., Usupaev, S., Picozzi, M., Di Giacomo, D., Augliera, P., D'Alema, E., Milkereit, C., Moldobekov, B., Zschau, J. (2010): Site Effects Assessment in Bishkek (Kyrgyzstan) Using Earthquake and Noise Recording Data. - Bulletin of the Seismological Society of America, 100, 6, 3068-3082

DOI: 10.1785/0120100044

Site effect assessment in Bishkek (Kyrgyzstan) using earthquake and noise recording data

S. Parolai[1], S. Orunbaev[3], D. Bindi[2,1], A. Strollo[1,4], S. Usupaev[3], M. Picozzi[1], D. Di Giacomo[1,4], P. Augliera[2] , E. D'Alema[2], C. Milkereit[1], B. Moldobekov[3] and J. Zschau[1]

[1]Deutsches GeoForschungsZentrum GFZ, Section 2.1, Telegrafenberg, 14473 Potsdam, Germany

[2]Istituto Nazionale di Geofisica e Vulcanologia, Via Bassini 15, 20133 Milano Italy

[3]Central Asian Institute for Applied Geosciences, Timur Frunze rd.73/2, 720027, Bishkek, Kyrgyz Republic

[4]Institute of Geosciences, Universität Potsdam, Karl-Liebknecht Strasse, 14476 Potsdam, Germany

Site effect assessment in Bishkek (Kyrgyzstan) using earthquake and noise recording data

S. Parolai[1], S. Orunbaev[3], D. Bindi[1,2], A. Strollo[1,4], S. Usupaev[3], M. Picozzi[1], D. Di Giacomo[1,4], P. Augliera[2] , E. D'Alema[2], C. Milkereit[1], B. Moldobekov[3] and J. Zschau[1]

[1]Deutsches GeoForschungsZentrum GFZ, Section 2.1, Telegrafenberg, 14473 Potsdam, Germany
[2]Istituto Nazionale di Geofisica e Vulcanologia, Via Bassini 15, 20133 Milano Italy
[3]Central Asian Institute for Applied Geosciences, Timur Frunze rd.73/2, 720027, Bishkek, Kyrgyz Republic
[4]Institute of Geosciences, Universität Potsdam, Karl-Liebknecht Strasse, 14476 Potsdam, Germany

Abstract

Kyrgyzstan, which is located in the collision zone between the Eurasian and Indo-Australian lithosphere plates, is prone to large earthquakes as shown by its historical seismicity. Hence, an increase in the knowledge and awareness of local authorities and decision makers of the possible consequence of a large earthquake, based on improved seismic hazard assessments and realistic earthquake risk scenarios, is mandatory to mitigate the effects of an earthquake. To this regard, the Central Asia Cross-Border Natural Disaster Prevention (CASCADE) project aims to install a cross-border seismological and strong motion network in Central Asia and at support microzonation activities for the capitals of Kyrgyzstan, Uzbekistan, Kazakhstan, Tajikistan and Turkmenistan. During the first phase of the project, a temporary seismological network of 19 stations was installed in the city of Bishkek, the capital of Kyrgyzstan. Moreover, single station noise recordings were collected at nearly 200 sites. In this study, the site amplifications occurring in Bishkek are assessed by analyzing 56 earthquakes extracted from the data streams acquired continuously by the network, as well as from the single station noise measurements. A broad-band amplification (starting at ~ 0.1 and

0.2 Hz), is shown by the Standard Spectral Ratio (SSR) results of the stations located within the basin. The reliability of the observed low frequency amplification was validated through a time-frequency analysis of de-noised seismograms. Discrepancies between Horizontal-to-Vertical Spectral Ratio (HVSR) and SSR results are due to the large amplification of the vertical component of ground motion, probably due to the effect of converted waves. The single station noise results, once their reliability was assessed by their comparison with the earthquake data, have been used to produce the first fundamental resonance frequency map for Bishkek, whose spatial variation shows a good agreement with the presence of an impedance contrast within the Tertiary sedimentary cover.

Introduction

Kyrgyzstan, which is located in the collision zone between the Eurasian and Indo-Australian lithosphere plates, is prone to large earthquakes as shown by its historical seismicity. In particular, between the end of the 19th and the beginning of the 20th centuries, several destructive earthquakes occurred in Kyrgyzstan, such as the Belovodski earthquake of August 3, 1885 (maximum intensity IX), that struck the city of Kara-Balti just west of Bishkek (Bishkek developed as a city during the 20th century), and the Ms=8.2 Kemin earthquake of January 3, 1911 (Figure 1). This earthquake killed several hundred people and had a strong impact on the environment, triggering several mudflows and landslides (Abdrakhmatov et al., 2003). Recently, on October 5, 2008, a magnitude 7.0 event (Figure 1) occurred along the border triangle between Kyrgyzstan, Tajikistan, and China. This earthquake caused the loss of about 350 lives, confirming the urgency of developing international programs for earthquake risk mitigation in Kyrgyzstan.

The occurrence of close and large earthquakes makes Kyrgyzstan the region with one of the highest seismic hazard in the world (Zhang, 1999). The probabilistic seismic hazard maps at regional scale computed for Kyrgyzstan (Abdrakhmatov et al., 2003) show a peak ground acceleration of up to 4.5 m/s^2 with a probability to be exceeded of 10% over the next 50 years, confirming the very high hazard of the region.

The high risk level in Kyrgyzstan is not only dictated by the high level of the seismic hazard, but it is also a function of the vulnerability of buildings. The workshop held in Almaty (Kazakhstan) on October 1996 (Khalturin and Tucker, 1997) on the "Strategies for urban earthquake risk management for the Central Asian Republics" pointed out that the seismic resistance of Soviet-era buildings was significantly lower than was officially proclaimed. Analysing the devastating effects of the 1988 Armenian and 1995 Sakhalin earthquakes, the authors observed that "*Millions of people in Central Asia live in the same types of buildings*

as those collapsed in Armenia and Sakhalin. If an earthquake of the same size occurs near one of the Central Asian capitals, the tragedies of Leninakan, Spitak, and Neftigorsk will be repeated on a much bigger scale, unless urgent measures are taken". The assessment of the urban earthquake risk of two Central Asian cities, i.e. Bishkek (Kyrgyzstan) and Tashkent (Uzbekistan), has been the subject of a NATO Science for Peace Project funded in 2001 (Erdik et al., 2005). The project evaluated the seismic hazard for the two cities accounting to a first-order approximation of the potential site amplification effects, quantifying the building vulnerability and, finally, evaluating the urban earthquake risk. The project provided the indication that the expected number of night-time casualties in Bishkek under exposure to earthquake with a 2% probability of exceedance in 50 years is about 34.000. Moreover, about 90.000 people are expected to suffer injuries that will need to be treated at hospitals.

The effect of a large earthquake close to a major city can actually cause not only a large number of casualties, but also an economic collapse. Hence, an increase in knowledge and awareness of local authorities and decision makers of the possible consequence of a large earthquake is mandatory to mitigate the effects of an earthquake (building collapse, damage to lifelines, activation of landslides that can affect industrial, chemical or nuclear waste storage sites, and other sites of importance for security) and can only be based on improved seismic hazard assessments and realistic earthquake risk scenarios. To accomplish this task, however, hazard assessment should be performed only after having calibrated the required ground motion empirical equation with data collected in the area and having considered the effect of shallow geological material in modifying earthquake ground motion. To this regard, the Central Asia Cross-Border Natural Disaster Prevention (CASCADE) project, financed by the German Federal Foreign Office, aims to install of a cross-border seismological and strong motion network in Central Asia, and to carry out microzonation studies in the capitals of Kyrgyzstan, Uzbekistan, Kazakhstan, Tajikistan and Turkmenistan. During the first phase of the project, a temporary seismological network of 19 stations was installed in the city of

Bishkek, the capital of Kyrgyzstan, located over thick Quaternary and Tertiary deposits (Figure 1, top). Moreover, noise recordings were collected by means of nearly 200 single station noise measurements as well as a number of array configurations. Measurements were taken in the actual urban area of the town, as well as in the area to the south where the basin is bordered by the active Issyk-Ata fault. In this study, we analyse the earthquake and noise data for identifying spatial ground motion variability. The reliability of the observed low frequency amplification was validated through a time-frequency analysis of de-noised seismograms . Finally, the single station noise results, once calibrated by comparison with the earthquake data results, have been used to produce the first fundamental resonance frequency map for Bishkek.

Geological and geophysical setting

The town of Bishkek (Figure 1) is located in one of the largest depression of the Northern Tien Shan, the Chu basin. This basin is bounded by the Kyrgyz Range to the south and the Chu-Lli mountains in the north. The Kyrgyz Range is mainly made up of Ordovician granite and fine-grained Devonian sedimentary rocks. It is cut by several short, irregular imbricate thrust faults that are laterally truncated by strike slip faults (Bullen et al., 2001). The Paleozoic bedrock is thrust northward over ~4 km of Cenozoic molasse at the margin of the Chu basin. The latter is some 50 km wide and 150 km long. The deformation front is stepped northward into the Chu basin, exposing a thick succession of Neogene strata along the Issyk-Ata fault, located ~10 km north of the basin margin structure. Below the urban area of Bishkek the Paleozoic basement depth is expected to generally decrease from the north (~1 km) to south (~3 km). However, in the south west of the study area, a local deepening of the basement to more than 3 km can be expected. The seven thick Tertiary formations overlying

the Paleozoic bedrock are respectively made, from bottom to top, of siltstones and sandstones (Kokturpak and Kokomeren Formations, respectively), claystones (Sera Firma Formation), mudstones (Dzhel'dysu Formation), sandstones and pebbly conglomerate (Saryagach Formation), mudstones and sandstones (Chu Formation), and coarse-pebble conglomerate (Sharpyldak Formation) (Bullen et al., 2001). In particular, the shallowest part of the Sharpyldak formation is made up of poorly sorted, matrix supported, fan conglomerates with granitic boulders as large as 1 m in diameter. Quaternary sediments with a thickness of 200-300 m overlie the Cenozoic deposits. To the south of the studied area, alluvial material made up of rubble and gravel with a thickness of between 15 and 40 m outcrops. The same material can be found within the urban area along the major rivers. In the southern half of the Bishkek territory, alluvial gravels, rubble and sandy material (with a thickness ranging between 25 and 50 m) constitute the shallowest geological layers. The lower Quaternary sediments made up of rubbly-bench gravel with clay-sand lenses and break stone bench gravel outcrop in the northern part of the town. Occasionally, older Quaternary alluvial proluvial of rubbly-bench gravel with clay-sand lens outcrop in the northern part of the town.

Since information about the S-wave velocity in the shallow sedimentary layers was not available, an array measurement of seismic noise was carried out. We used all the available 19 stations and the array was installed near the position of station BI08 of the temporary seismological network (Figures 1, top and 2a). Seismic noise was recorded simultaneously by all stations for a few hours at 500 samples per second sampling rate. Simultaneous recordings of one hour of noise were used and divided in 60 second length windows. Only the vertical component was analyzed. Recordings were corrected for the instrumental response, considering the calibration parameters of each sensor, and the data have been analysed using the Extended Spatial Autocorrelation method (ESAC) (Ohori et al., 2002; Okada, 2003; Parolai et al., 2006; Parolai et al., 2007). The obtained dispersion curve (Figure 2b), ranging between 3 to 13 Hz, shows a normal dispersive behaviour. The highest frequencies already

show a quite high Rayleigh wave phase velocity (600 m/s) that increases up to 1100 m/s for the lower frequencies. These values are consistent with the existence of stiff Quaternary alluvial material made up of rubble and gravels in the study area. Due to the simplicity of the dispersion curve a simplified linearized inversion (e.g. Parolai et al., 2006 and reference therein) was carried out.

The obtained model (Figure 2c) shows a regular increase of velocity with depth, starting from nearly 600 m/s in the shallowest layers (0-25 m depth) and increasing to 1380 m/s at the deepest ones. Note that the investigated depth range lies within the Quaternary sedimentary cover and it is reliable (as estimated by resolution matrix analysis here not reported) down to nearly 200 m depth.

Earthquake data

From August 16 2008 a temporary seismological network was installed in Bishkek (Figure 1, top). The network consisted of fifteen EDL 24bit acquisition systems equipped with thirteen short-period Mark-L4-C-3D sensors, one Güralp CMG-ESPC 60 and a IO-3D 4.5 Hz sensor, and four Reftek-130 digitizers connected to Lennartz LE3D-5s. Stations were operated in continuous mode until the middle of November 2008 and were installed in the cellars of public buildings or private houses in order to cover the urban area of Bishkek. One station (BI04) was installed in the Kyrgyz range with the aim of having a reference station for the site effect estimation analysis. However, this station, for logistic problems, could only be installed over a thin layer of detritus (mainly rubble and gravel) deposited on the slope of the hill. Furthermore, due to problems with power supply and the extremely low temperatures, it only worked for one month. All stations recorded at 100 samples per seconds.

From the continuous data streams recorded by the network, the recordings of 56 earthquakes were extracted using a slightly modified version of the procedure proposed by Galiana-Merino et al. (2008). The distribution of their epicentres is shown in Figure 1, with Table 1 listing the main parameters of the earthquake sources. The data set includes 50 crustal earthquakes with magnitude between Ml=1.6 and Mw=6.6, that occurred at distances between about 35 and 1527 km from station BI08. The recordings of 5 deep earthquakes, with magnitude between mb=5.1 and Mw=5.8 that occurred in the Pamir-Hindu Kush seismic zone, are also included in the data set. Finally, a magnitude Mw=7.3 earthquake that occurred at a distance of 5685 km in the Sea of Okhotsk (Russia) at a depth of 492 km (not shown in Figure 1), completes the data set.

The different energy content of the earthquake recordings (due to different hypocentral distances and magnitudes) allows us to widen the frequency range investigated. Figure 3 shows the recordings of a mb = 4.6 earthquake that occurred 144 km from station BI08 (event 1 in Table 1). Note the different waveforms depending on the position of the station. The following analyses were performed considering frequencies with a signal-to-noise (SNR) ratio larger than 3 (estimated by considering the Fast Fourier Transform (FFT) of a noise window as wide as the signal window). Based on the results of previous studies (e.g. Strollo et al., 2008a,b), that showed that the short period sensors provide reliable seismic noise recordings down to frequencies of ~0.1 Hz, no a priori choice of the investigated frequency band was carried out. We corrected the recordings for the instrumental response and the spectra were smoothed using a triangular window equal-spaced in logarithm scale (10% of the central frequency).

Horizontal-to-Vertical spectral ratio (HVSR)

The HVSR (Lermo and Chavez-Garcia, 1993) method belongs to the class of so-called non-reference site methods (Bard, 1995). Although there is not a theoretical basis demonstrating that HVSR is an estimate of the site transfer function, and Parolai and Richwalski (2004) showed using numerical simulations that it underestimates the amplification at frequencies larger than the fundamental one, it is generally considered useful for estimating the fundamental resonance frequency of a site (e.g. Field and Jacob, 1995).

After having tested several criteria for the signal window selection (including fixed window length and energy criteria), the data analysis was carried out using windows of fixed 50 second length. This was due to the requirement of including enough low-frequency cycles that, due to the thickness of the sedimentary cover in the area, were expected to be of interest for estimating the resonance frequency of the investigate sites. Figure 3 shows examples of windows of signal selected for the following analysis.

The results in Figure 4 and 5 (first column) show that HVSR for the stations installed in the northern part of the town over the older Quaternary material (Figure 1, BI01, BI05, BI14, BI15, BI16, BI17, BI18), clearly show a first resonant peak at ~0.2 Hz. Although the HVSR were computed considering the two horizontal components separately, Figures 4 and 5 show the results only for the east-west (EW) component, as similar trends are also obtained for the North-South (NS) component (not shown). After a narrow through around 0.3 Hz, the HVSR is almost flat and then shows a bump starting from between 2-3 Hz up to 10 Hz (in the case of station BI17). The stations located in the central part of the urban area (BI02, BI08, BI09, BI11, BI12, BI13, BI19) show a smaller-amplitude low-frequency peak (between 0.1 and 0.2 Hz) followed by a very large trough and then by a nearly flat HVSR. The stations located at the southern margin of the investigated area, where the Tertiary material makes a tectonic

contact with Quaternary sediments (BI03, BI06, BI07 and BI10), show a peculiar behaviour strongly dependent on small scale changes in the surface geology. While the HVSR of BI10 is nearly flat up to 1 Hz and then rapidly increases, showing a large peak at 7 Hz, the HVSR of BI06 resemble those of the station located in the central part of the town (nearly flat with a 0.3 Hz trough). A similar HVSR shape is shown by station BI07 and BI03. Finally, it is worth noting that the HVSR at station BI04 (Figure 5), which was supposed to be a possible reference station, can be considered flat only up to nearly 2 Hz. At higher frequencies, large amplifications are shown with a main peak at ~ 5 Hz.

HVSR of de-noised seismograms

The reliability of the low (0.1-0.2 Hz) frequency peak in the HVSR, being calculated for frequencies with high SNR ratio and its relation with the arrival of the larger amplitude phases (S-wave train) was evaluated by de-noising the seismograms using a S-transform based approach (Parolai, 2009) and analysing the distribution of energy on the time frequency plane. The S-transform (Stockwell et al, 1996) is a time-frequency localization spectral method similar to the short-time Fourier transform (Gabor, 1946), but with a Gaussian window whose width scales inversely, and whose height scales linearly, with the frequency.

The S-transform of a function $h(t)$ is defined as:

$$S(\tau, f) = \int_{-\infty}^{\infty} h(t) \frac{|f|}{\sqrt{2\pi}} e^{-\frac{(\tau - t)^2 f^2}{2}} e^{-i2\pi ft} dt \qquad (1)$$

Where t is the time, f the frequency and τ is a parameter that controls the position of the Gaussian window along the t-axis. Recently, Parolai (2009) applied to the S-transform coefficients the continuous thresholding function proposed by Yoon and Vaidyanathan (2004) that was shown to outperform the traditional soft and hard-thresholding schemes and can be

adapted to the characteristic of the input signal for de-noising seismograms corrupted by noise. The resulting method was found to be very effective, in particular when compared with standard filtering approaches, and hence, in this study, the seismic recordings have been de-noised following the Parolai (2009) procedure. The Fourier spectra of the de-noised signal have been in turn used to calculate the HVSR. This approach offers two main advantages:

1) The HVSR is calculated only on signal, avoiding the subjective choice about the frequency band to be used on the basis of an average SNR ratio.
2) The Fourier spectrum of the filtered signal might be estimated by integrating the $S(\tau, f)$ of the filtered signal along the time axes, also using frequency dependent time window of integration. This would allow a comparison, if required, for an equal number of cycles of the frequency content.

In this study, the Fourier transform of the spectrum was obtained by integrating for the whole duration of the seismogram. Finally, the HVSR was calculated between the integrated raw Fourier spectra.

Figure 6 shows, as an example, the EW and Z recordings and their correspondent S-transforms of event 1 in Table 1. The filtered seismograms and their S-transforms are also shown. We note that just after the S-waves, an arrival with high energy occurs with a frequency around 0.2 Hz that was identified as the resonance frequency of the site, on the EW component of the ground motion, but not observable on the vertical one. The Fourier spectrum of the de-noised EW component signal (Figure 7) clearly shows a large amplification peak at around 0.2 Hz. Interestingly, after applying the de-noising procedure, signal content down to 0.06 Hz can be observed. The HVSR for this station, determined by combining spectral ratios from four earthquakes (events 1, 6, 15, and 36 in Table 1), with different magnitudes and occurring at different hypocentral distances are shown in Figure 8. Although affected by a large scatter due to the calculation of the spectral ratios from raw spectra, the trend of the HVSR shows, in agreement with the results shown for this station in

Figure 4, a clear peak at around 0.2 Hz. These results indicate that the low frequency peak in HVSR is due to the amplification of the horizontal component of ground motion occurring just after the S-wave arrival. They also confirm the reliability of the HVSR results obtained for these low frequencies, independent of the SNR ratio threshold chosen and the length of the window used for the analysis.

Standard Spectral Ratio

The Standard Spectral Ratio technique (SSR) (e.g. Borcherdt, 1970; Parolai et al., 2000) consists of comparing records at nearby sites, using one as the reference. It is assumed that records from the reference site (in general, a station installed on outcropping hard bedrock) contain the same source and propagation effects as records from the other sites. Therefore, the spectral ratio directly provides the site response.

Although station BI04 was not found to be an ideal reference site, it might still be used as a reference station for the frequency range lower than 2 Hz. In fact, over this frequency range, the HVSR results show values of nearly one. Furthermore, the distance between this station and the other stations of the network is short enough to assume that only minor propagation effects are affecting the SSR results over this frequency range. Due to the instrumental problems of station BI04, only 7 events (see Table 1) could be used for estimating the SSR. Since stations BI05 and BI12 have not recorded the events available for BI04, the SSR analysis cannot be carried out for these two stations. Results obtained for the East-West (EW) and vertical (Z) components of ground motion are shown in Figure 4 (third and fourth column, respectively). Differently from the HVSR, results of all the stations in the basin show very similar behaviour for the horizontal component SSR. In particular, a broad amplification is observed with clear distinct peaks between 0.1 and 0.2 Hz (increasing from South to North), 0.4 Hz and between 1 and 2 Hz. Occasionally, some stations (e.g. BI03, BI15) also

show distinct amplification peaks at 0.6-0.7 Hz. Above 2 Hz, the large de-amplification effect is due to the amplification occurring at the reference site. Stations BI10, BI07 and BI06, located at the southern margin of the basin, show different behaviours. BI10 is nearly flat with a small amplification at around 1.5 Hz. BI07 and BI06 show only moderate amplification, increasing nearly linearly from the lower frequencies up to 1-2Hz. The following decaying trend is not reliable due to the amplification affecting the reference station over that frequency range.

The differences between the HVSR and SSR results can be easily explained by considering the SSR results obtained by analysing the vertical component of ground motion. In fact, the vertical component SSR of the stations within the basin (Figure 4, fourth column) are showing large amplifications with peaks at frequencies (~0.3-0.5 Hz) systematically larger than those observed on the horizontal component results. These peaks are particularly large, even occasionally becoming predominant, for the stations BI13, BI08, BI09, BI11 located on the younger Quaternary sediments outcropping in the southern part of the urban area. The positions of these peaks coincide with the spectral troughs in the HVSR. Considering that

- the HVSR of the reference station is not affected by the narrow spectral troughs at 0.3-0.5 Hz (indicating that no amplification of the vertical component in that frequency range take place outside of the basin), and
- the role of surface waves might be ruled out, since the amplitude peaks in the low frequency range are occurring at different frequencies on the vertical and horizontal components,

the results might be interpreted considering the effect of converted waves on the recorded ground motion. In fact, previous studies (e.g. Takahashi et al., 1992; Parolai and Richwalski, 2004) showed that at the boundaries between shallow geological layers, significant P-to-S conversion and S-to-P conversion can take place and, therefore, affect the HVSR results.

Figure 9 (left) shows the vertical, radial and transverse component seismograms at station BI13 (strongly affected by amplification on the vertical component) of event 1 (Table 1). It is remarkable how from just a few tenths of seconds before the S-wave arrival the vertical component shows significant ground motion lasting for several seconds. By contrast, Figure 9 (right) shows the vertical, radial and transverse component seismograms at the same station of an mb = 5.2 earthquake that occurred at ~800 km hypocentral distance (ID 15 in Table 1), that is much farther than the first example. Only the first tens of seconds before the S-wave arrival are shown. In this case, it is clear how the first trough and the second peak in the vertical component are also observed, although shifted, on the radial one. The large amount of energy in the radial component recordings in the P-wave window for a nearly vertical incidence event suggests that wave conversion takes place. The shift between peaks and troughs observed for different components might account for the different wave velocity propagation.

Formatiert: Nicht Hervorheben

Formatiert: Nicht Hervorheben

Formatiert: Nicht Hervorheben

Noise data

Seismic noise was collected at 196 sites in the urban area of Bishkek and in the southern surroundings where Quaternary layers overlap the folded Tertiary material (Figure 1). One EDL 24 bit acquisition system, equipped with a short-period Mark-L4-C-3D sensor, was used for the measurements. Noise recorded in continuous mode by the temporary seismological network was also included in the analysis. Depending on the station, ten to thirty 60 second noise windows have been considered for each measurement points. Time series have been tapered at both ends with a 5% cosine taper and their Fast Fourier Transform (FFT) calculated. The FFT have been smoothed using a Konno-Ohmachi window (Konno and Ohmachi, 1998) fixing the parameter b that determines the degree of smoothing to 40. For

each 100 second window the horizontal-to-vertical spectral ratio (NHVSR) was computed (Nogoshi and Igarashi, 1970; Nakamura, 1989) and the logarithmic average of the NHVSR estimated. Figure 4 (second column) shows the NHVSR computed for sites where the temporary seismic network was installed, considering the pre-event noise windows. A generally good agreement between the fundamental frequency of resonance obtained from the HVSR (first column) and the NHVSR (second column) is observed. The results presented in Figure 10 show that in the urban area of Bishkek, north of the outcropping Tertiary material, the fundamental resonance frequency of soil spans, consistent with the SSR results, from nearly 0.3 Hz to the North to ~0.1 Hz in the South. The general decrease of the fundamental resonance frequency from North to South is consistent with the geological structure of the basin, which shows an increase in the thickness of the Quaternary and Tertiary sedimentary cover towards the south (Bullen et al., 2001, their Figures 4 and 5). Considering the high value of the S-wave velocity characterising the shallow Quaternary layers (Figure 2), the low value of the resonance frequency might be indicative of a deep impedance contrast, likely to exist between the Sharpyldak and Chu formations. The lower-resonance frequencies observed in the south-western part of the area are consistent with a thickening of the sedimentary cover as proposed by Bullen et al. (2001) and in the references therein.

The occasionally observed very low frequency peak (lower than 0.1 Hz) in the southernmost part of the investigated area could be related (similarly to the fundamental resonance frequency in the urban area) to the contact between the Sharpyldak and Chu formation. Note that in this area, due to the geological structure forming a sincline in the Tertiary material, the thickness of the Sharpyldak formation can reach values even larger than those below the urban area (Bullen et al., 2001, their Figure 5). However, due to the technical limitation of the used geophone, we cannot consider fully reliable results obtained below 0.1 Hz (Strollo et al., 2008,a,b) and we therefore refrain from analysing them too deeply to avoid misinterpretation. Finally, the increase of the fundamental frequency of resonance in the southernmost part of

the investigated area, toward the Kyrgyz Range, is in agreement with the expected lateral variations due to an outcropping of the Chu and Sharpyldak formations, which generates a small basin made up of Quaternary material (Bullen et al., 2001, their Figure 5).

In conclusion, we remark that although the NHVSR shape, especially at intermediate frequencies, might be different from the SSR one at the corresponding stations, their variability is consistent with that of the SSR. That is, differently from what we observed by comparing the HVSR results with the SSR ones, stations showing similar SSR also show similar NHVSR

Discussion and Conclusions

In this study we analysed earthquake and seismic noise recordings collected in the area of Bishkek (Kyrgyzstan). Results showed that significant amplification (~5) affect the ground motion in the case of earthquakes. Of particular relevance is the wideness of the frequency band that can be amplified, ranging from nearly 0.1 Hz to more than 2 Hz. Several peaks can be distinguished in the calculated site responses that may be a result of the complex geological setting (with several overlapping units) of the area. Considering both the high velocities estimated by means of array measurements in the shallow sedimentary cover and its thickness, it is likely that the wideness of the amplified frequency band might indicate a small damping of ground motion, which may be due to the stiffness of the material through which the waves propagate.

Recently, the slope of topography was suggested (Wald and Allen, 2007) as proxy parameter for estimating Vs30 and therefore for soil classification in terms of site effects. On one hand, we found that the slope of the topography in the studied area (ranging between 0.0015 in the northern part of the basin and 0.3 in the Kyrgyz range), computed using the GTOPO30

topographic model (see Data and Resources), is a reliable proxy for estimating the shear-wave velocity in the shallowest 30 meters (Vs30) of the Quaternary layer covering the central and southern part of Bishkek, since it indicates velocities between ~400 m/s and 760 m/s (NEHRP class C), compatible with the S-wave velocity profile obtained by our array measurements. On the other hand, the velocity for the northern part seems to be underestimated, since the velocities estimated from the slope correspond to class D, while neither the site response nor the local geology shows any significant variations. Moreover, note that station BI04, installed in the Kyrgyz range, that would be classified as NEHRP class B (rock site) was found to show significant amplification above 2 Hz. Finally, a site classification only based on Vs30 is not adequate to account for the broad-band site amplification, since it completely fails to describe the site amplifications occurring at frequencies smaller than 1 Hz.

We verified by a careful time-frequency analysis that the lowest frequency peak in the SSR and HVSR was to be ascribed to resonance occurring just after the S-wave arrival. However, we found significant differences between the SSR and the HVSR results at frequencies higher than the resonant one. As a possible mechanism responsible for this disagreement, after a careful and thorough analysis of several recordings, we propose the role of converted phases. Previous papers (e.g. Takahashi et al., 1992; Parolai and Richwalski, 2004) showed in fact that similar behaviour can be due to wave conversions when a large impedance contrast exists.

The single noise station measurements, once calibrated through a comparison with the earthquake data results, allowed us to enlarge the area of investigation improving also the spatial resolution. We found that, differently from the HVSR results, the spatial consistency of the NHVSR curves was equivalent to that of the SSR one. In particular, the fundamental resonance frequency was better evaluated using NHVSR than HVSR. This can be explained considering the different composition of the seismic noise (mainly dominated by surface waves) and the earthquake wavefields, where converted phases can affect the vertical

component of the ground motion at frequencies close to the fundamental resonance frequency of the site. Innovatively for the area, a first map of the fundamental resonance frequency of soil was calculated, showing that a large impedance contrast within the Tertiary sedimentary cover might be responsible for the first amplification peak of ground motion. However, considering the broad band amplification shown by the SSR results, the fundamental resonance frequency map can be considered as providing the lower bound of frequency from which amplification starts.

Since our results are based only on weak motion data, future projects should be devoted to investigating soil behaviour for the case of strong ground motion, both considering the geotechnical characteristic of the shallow geological material and the water table depth, and including the recordings of strong motion data. To this regards, future projects, as a continuation of the CASCADE one, will aim at the installation of a strong motion network in Bishkek. Finally, the obtained results will be considered, while re-assessing the seismic hazard and risk for Bishkek, in the framework of the Global Earthquake Model (www.globalquakemodel.org) program, contributing to a harmonised risk assessment in Central Asia.

Data and resources

The following data and software have been used in this study:

GTOPO30 - global digital elevation model (DEM) with a horizontal grid spacing of 30 arc seconds: http://eros.usgs.gov/#/Find_Data/Products_and_Data_Available/gtopo30_info

last access on February 2010

GMT – Generic Mapping Tool (Wessel and Smith, 1991) : http://gmt.soest.hawaii.edu/

last access on February 2010

ISC catalog - http://www.isc.ac.uk/

last access on February 2010

Acknowledgments

We are very grateful for the collaboration and support given to us during the survey measurements and the data collection by the people of Bishkek. M. Pilz estimated the slope of topography and R. Milkereit improved Figures. We thank J. Tokmulin and U. Abdybachaev for the help during the field work. A. Meleshko digitized the geological map. Dr. K. Fleming kindly revised our English. Instruments were provided by the Geophysical Instrumental Pool, Potsdam (GIPP). This research has been developed within the project “Cross-Border Natural Disaster Prevention in Central Asia” funded by Federal Foreign Office of Germany, and supported by the Global Change Observatory Central Asia of the GFZ.

References

Abdrakhmatov, K., H-B. Havenith, D. Delvaux, D. Jongmans and P. Trefois (2003). Probabilistic PGA and Arias Intensity maps of Kyrgyzstan (Central Asia), *Journal of Seismology* **7**, 203-220

Bard, P.-Y. (1995). Effects of surface geology on ground motion: recent results and remaining issues, in 10th European Conference on Earthquake Engineering, Duma (Editor), Balkema, Rotterdam, 305–323.

Borcherdt, R. D. (1970). Effects of local geology on ground motion near San Francisco Bay, *Bull. Seism. Soc. Am*. **60**, 29–61.

Bullen, M. E., D. W. Burbank, J.J. Garver,., and K. Ye. Abdrakhmatov (2001). Late Cenozoic tectonic evolution of the northwestern Tien Shan: New Age Estimates for the initiation of mountain building, *Geological Soc. of am. Bull*. **113**, 1544-1559.

Erdik M., T. Rashidov, E. Safak, A. Turdukulov (2005). Assessment of seismic risk in Tashkent, Uzbekistan and Bishkek, Kyrgyz Republic, *Soil Dynamics and Earthquake Engineering* **25**, 473–486

Field, E. H., and K. H. Jacob (1995). A comparison and test of various site response estimation techniques, including three that are non reference-site dependent*, Bull. Seism. Soc. Am.* **86**, 991–1005

Gabor D. (1946). Theory of communications, *Journal of Institution of Electrical Engineering* **93**, 429-457

Galiana-Merino, J. J., J. L. Rosa-Herranz, and S. Parolai (2008). Seismic P Phase Picking Using a Kurtosis-Based Criterion in the Stationary Wavelet Domain, *IEEE Transactions on geoscience and remote sensing* **46**(11), 3815-3826, doi: 10.1109/TGRS.2008.2002647.

Khalturin V. and B. Tucker (1997). Lessons from Armenia and Sakhalin for Central Asia, Report of the October 1996 Workshop in Almaty (Kazakhstan) on "Strategies for Urban Earthquake Risk Management for the Central Asian Republics", *IRIS Newsletter*

Konno, K., and T. Ohmachi (1998). Ground-motion characteristics estimated from spectral ratio between horizontal and vertical components of microtremor, *Bull. Seismol. Soc. Am*. **88**, 228–241.

Lermo, J., and F. J. Chavez-Garcia (1993). Site effect evaluation using spectral ratios with only one station, *Bull. Seismol. Soc. Am*. **83**, 1501–1506.

Nakamura, Y. (1989). A method for dynamic characteristics estimations of subsurface using microtremors on the ground surface, *Q. Rep. Railway Tech. Res. Inst. Japan* **30**, 25–33.

Nogoshi, M., and T. Igarashi (1970). On the propagation characteristics of microtremors, *J. Seism. Soc. Japan* **23**, 264–280 (in Japanese with English abstract).

Ohori, M., A. Nobata, and K. Wakamatsu (2002). A comparison of ESAC and FK methods of estimating phase velocity using arbitrarily shaped microtremor analysis, *Bull. Seism. Soc. Am.* **92**, 2323-2332.

Okada, H. (2003). The microtremor survey method. Geophysical monograph series 12, American Geophysical Union, Washington

Parolai, S., D. Bindi, and P. Augliera (2000). Application of the generalized inversion technique (GIT) to a microzonation study: numerical simulations and comparison with different site-estimation techniques, *Bull. Seismol. Soc. Am.* **90**, 286–297.

Parolai, S., and S. M. Richwalski (2004). The importance of converted waves in comparing H/V and RSM site response estimates, *Bull. Seismol. Soc. Am.* **94**, 304–313.

Parolai, S, S.M. Richwalski, C. Milkereit, and D. Faëh (2006). S-wave velocity profiles for earthquake engineering purposes for the Cologne area (Germany), *Bull Earth. Eng*. **4**, 65–94.

Parolai, S., M. Mucciarelli, R. Gallipoli, S.M. Richwalski, and A. Strollo (2007). Comparison of Empirical and Numerical Site Responses at the Tito Test Site, Southern Italy, *Bull. Seism. Soc. Am.* **97**, 1413-1431.

Parolai, S. (2009). Denoising of Seismograms Using the S Transform, *Bull. Seism. Soc Am*. **99**, 226 – 234

Stockwell, R.G., L. Mansinha,, and R.P. Lowe (1996). Localization of the Complex Spectrum: The S Transform, *IEEE Trans. Signal. Process*. **44**, 998-1001

Strollo A, S. Parolai, K.H. Jäkel, S. Marzorati, and D. Bindi (2008a). Suitability of short-period sensors for retrieving reliable H/V peaks for frequencies less than 1 Hz, *Bull. Seism. Soc. Am*. **98**, 671–681, doi:10.1785/0120070055.

Strollo, A., D. Bindi, S. Parolai, and K.-H. Jaekel (2008b). On the suitability of 1 s geophone for ambient noise measurements in the 0.1–1 Hz frequency range: experimental outcomes, *Bull. Earthq. Eng*. **6**, 141–147, doi 10.1007/s10518-008-9061-x.

Takahashi, K., S. Ohno, M. Takemura, T. Ohta, Y. Sugawara, T. Hatori, and S. Omote (1992). Observation of earthquake strong motion with deep borehole: generation of vertical motion propagating in surface layers after S-arrival, *Proc. Of the 10Pth P World Conf. on Earthquake Engineering,* **3**, 1245-1250.

Wald, D. J. and T. I. Allen (2007). Topographic Slope as a Proxy for Seismic Site Conditions and Amplification, *Bull. Seism. Soc. Am.* **97**, 1379-1395; DOI: 10.1785/0120060267

Wessel, P., and W. H. F. Smith (1991). Free software helps map and display data, *EOS Trans. AGU* **72**, 441, 445-446.

Yoon, B. J., and P. P. Vaidyanathan (2004). Wavelet-based denoising by customized thresholding, *IEEE Int. Conf. On Acoustic Speech and signal processing (ICASSP)*, Montreal, May 2004.

Zhang P., Z. Yang. H. K Gupta, S.C. Bhatia, and KM. Shedlock (1999). Global seismic hazard assessment program (GSHAP) in continental Asia, *Annali di Geofisica* **42**, 1167–90

ID	Date	OT	Lat.	Lon.	h(km)	Mag(type)	Dist.(km)	BAZ(BI08)
1*	2008/08/21	17:19:54.40	42.1030	75.9650	10.0f	4.6(mb)	144.11	124.94
2*	2008/08/21	19:34:06.94	41.9300	75.8040	33.0	4.3(mb)	146.47	134.13
3*	2008/08/24	10:04:37.50	40.3610	72.9740	6.7	4.1(mb)	306.04	205.58
4*	2008/08/30	12:46:45.58	42.6966	84.1352	2.0	5.5(mb)	783.49	88.01
5	2008/09/01	04:24:31.02	37.3900	68.9000	2.0	5.4(mb)	773.29	220.10
6*	2008/09/02	20:49:40.28	43.5544	79.5439	230.4	4.9(mb)	413.45	77.44
7*	2008/09/05	04:57:52.58	36.5360	71.2910	188.0	5.3(mb)	755.18	202.60
8*	2008/09/06	05:47:39.9	36.4900	70.9300	18.1	5.8(Mw)	771.75	204.72
9	2008/09/10	07:55:01.24	42.5741	74.8174	18.8	2.0(Ml)	38.86	143.21
10	2008/09/13	13:40:28.34	42.5330	74.5599	17.8	2.7(Ml)	35.79	176.49
11	2008/09/13	18:18:41.02	42.5314	74.5694	18.0	2.8(Ml)	36.03	175.27
12	2008/09/17	19:37:34.70	43.5990	78.5400	14.6	4.0(mb)	335.00	74.32
13	2008/09/20	02:41:18.30	42.0316	76.0275	19.9	1.9(Ml)	152.98	126.22
14	2008/09/20	04:15:51.86	42.2699	74.8597	100.0f	2.9(Ml)	70.27	157.52
15	2008/09/24	17:59:33.55	36.1530	71.2530	33.0	5.2(mb)	796.35	201.75
16	2008/09/26	22:23:22.50	40.6210	72.9360	37.0	4.2(mb)	281.47	208.62
17	2008/10/05	15:52:51.00	39.5330	73.8240	35.0f	6.6(Mw)	374.04	189.36
18	2008/10/05	16:11:10.42	39.5080	73.8880	33.0	5.6(mb)	375.99	188.47
19	2008/10/05	16:36:18.20	39.4920	73.8900	35.0f	5.1(mb)	377.72	188.41
20	2008/10/05	17:00:26.75	39.2640	73.8430	33.0	4.3(mb)	403.39	188.48
21	2008/10/05	18:27:39.40	39.4080	73.7320	35.8	5.1(mb)	389.04	190.20
22	2008/10/05	21:46:06.73	39.6940	73.7240	42.0	4.6(mb)	357.85	191.16
23	2008/10/07	16:43:29.80	42.1280	76.5860	27.0	4.0(mb)	186.68	114.94
24	2008/10/09	03:13:42.00	39.3770	73.9780	29.0	4.7(mb)	389.44	187.04
25	2008/10/09	14:43:19.40	39.4470	73.9340	122.7	4.9(mb)	382.18	187.74
26	2008/10/13	08:07:44.31	36.1870	71.0010	35.0f	5.1(mb)	800.69	203.37
27	2008/10/13	09:23:35.08	39.5800	73.8580	35.0f	5.0(mb)	368.44	189.04
28	2008/10/13	16:05:25.04	39.5000	73.8140	10.0f	5.0(Mw)	377.80	189.41
29	2008/10/13	17:16:09.99	38.5590	70.3380	11.0	5.3(mb)	594.10	217.90
30	2008/10/18	20:53:55.90	41.8000	81.0400	7.9	4.0(mb)	547.46	100.16
31	2008/10/18	21:15:24.75	42.6396	74.8415	4.1	1.6(Ml)	34.70	133.37
32	2008/10/19	01:27:15.50	41.4611	75.6909	14.2	3.1(Ml)	181.95	147.98
33	2008/10/20	19:58:01.73	41.7706	75.7582	35.0f	2.5(Ml)	157.06	139.69
34	2008/10/22	16:46:09.68	40.5960	78.0750	17.8	4.3(mb)	386.53	129.32
35	2008/10/23	05:50:45.60	39.4200	73.9340	210.0	4.8(mb)	385.16	187.68
36	2008/10/26	01:28:56.06	36.4900	70.6830	19.9	5.5(mb)	780.41	206.22
37	2008/10/28	01:05:23.05	42.9220	75.0563	15.0f	1.6(Ml)	43.28	79.81
38	2008/10/28	23:10:00.70	30.6390	67.3510	2.0	6.4(Mw)	1500.03	207.46
39	2008/10/28	23:17:23.89	30.3174	67.5086	14.0f	4.3(mb)	1527.21	206.40
40	2008/10/29	11:32:43.13	30.5980	67.4550	19.0	6.4(Mw)	1500.34	207.04
41	2008/11/01	05:48:01.33	42.7841	76.4509	26.3	3.7(mb)	156.61	92.21
42	2008/11/02	17:58:29.69	42.7940	76.4250	20.0	3.7(mb)	154.43	91.85
43	2008/11/04	14:22:23.92	39.4440	74.0550	35.0f	4.8(mb)	381.31	186.19
44	2008/11/04	15:46:52.91	39.2730	73.7260	35.0f	4.1(mb)	403.93	189.91
45	2008/11/06	14:23:51.80	39.4780	74.0170	16.8	4.8(mb)	377.90	186.74

46	2008/11/06	21:14:16.40	42.2980	75.2359	35.0f	2.2(Ml)	84.48	136.83
47	2008/11/07	09:21:17.26	39.3730	74.0110	26.9	4.6(mb)	389.56	186.62
48	2008/11/08	01:30:44.19	39.4790	73.9490	2.0	4.6(mb)	378.49	187.62
49	2008/11/09	02:48:04.54	42.3160	75.2200	2.0	2.1(Ml)	82.13	136.56
50	2008/11/09	03:31:29.76	42.4597	71.2813	35.0f	3.9(mb)	269.50	261.73
51	2008/11/09	19:22:49.43	39.4540	73.9650	18.3	4.5(mb)	381.07	187.36
52	2008/11/10	23:24:37.41	42.4345	74.6160	35.0f	1.8(Ml)	47.17	171.71
53	2008/11/13	20:52:08.87	39.5150	73.9600	35.0f	4.7(mb)	374.40	187.55
54	2008/11/18	00:15:12.28	39.5720	76.6380	492.0	3.5(mb)	405.19	153.55
55	2008/11/24	09:02:58.00	54.1800	154.3100	56.6	7.3(Mw)	5684.71	47.72
56	2008/11/26	16:41:23.36	39.3100	71.7970	10.0f	4.2(mb)	455.91	211.10

Table 1. List of earthquake parameters for the 56 events extracted from the continuous data streams and used in the analysis (Figure 1, bottom). The location and magnitude parameters are from the ISC catalogue (http://www.isc.ac.uk/index.html). The epicentral distances and back-azimuths to station BI08 are also reported. The symbol * indicates events used for the SSR method.

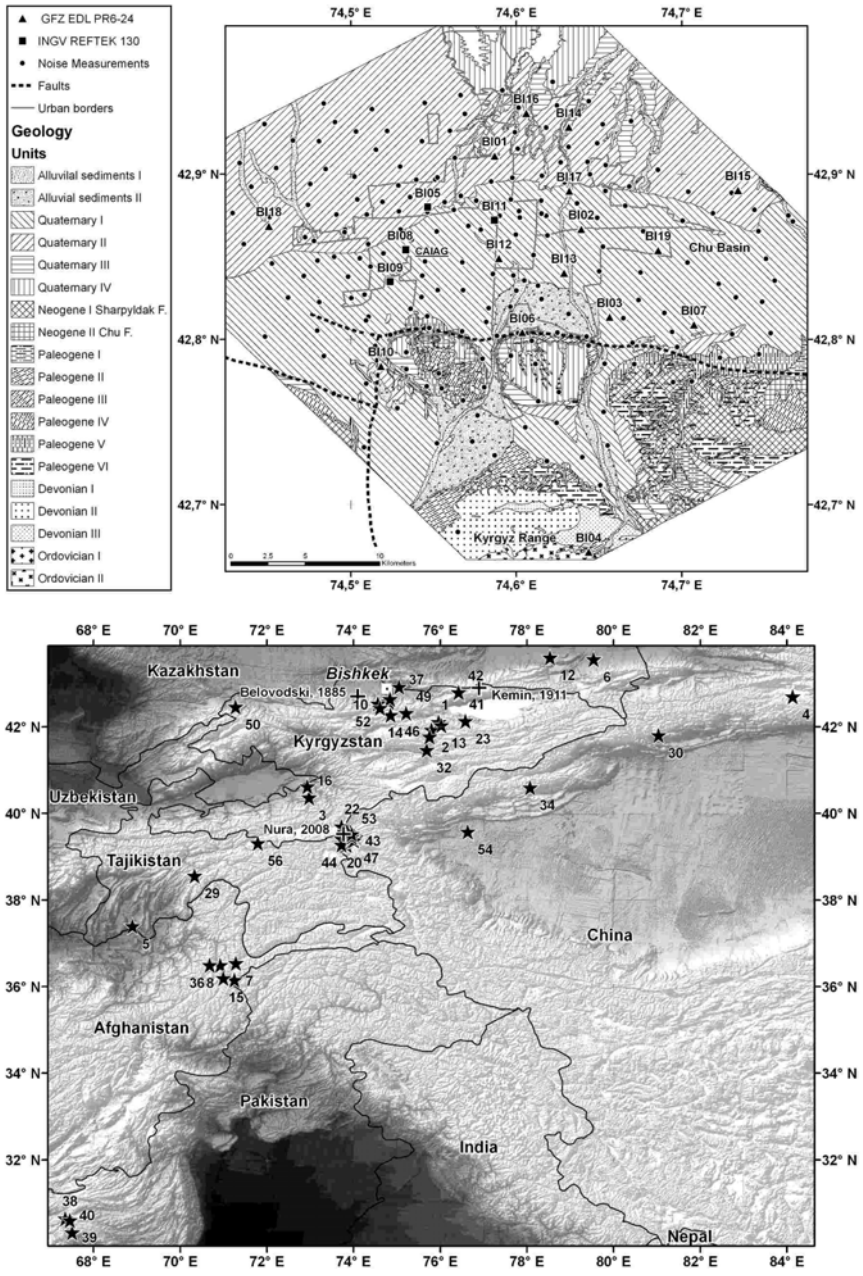

Figure 1: Top. Locations of the temporary stations (squares and triangles) installed in Bishkek and of the single station noise measurements (circles). A geological sketch of the area is also shown. Bottom. Epicenters (stars) of the earthquakes used in this study (Table 1). Event 55 in Table 1, occurred in the Sea of Okhotsk (Russia) is not shown in Figure. Crosses indicate the location of historical earthquakes mentioned in the text.

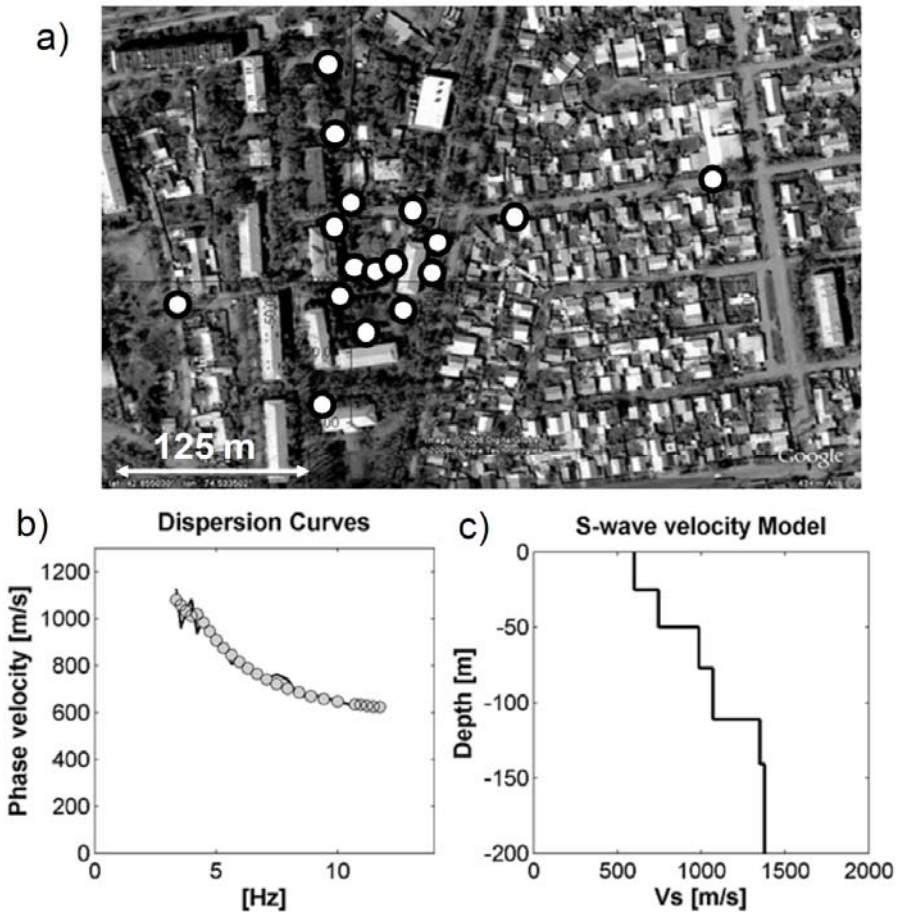

Figure 2: Results of the array inversion performed close to station BI08 (Figure 1). a) Array geometry (white circles); b) observed dispersion curve (black line) and reconstructed (gray circles); c) S-wave velocity model obtained by inverting the dispersion curve in panel b).

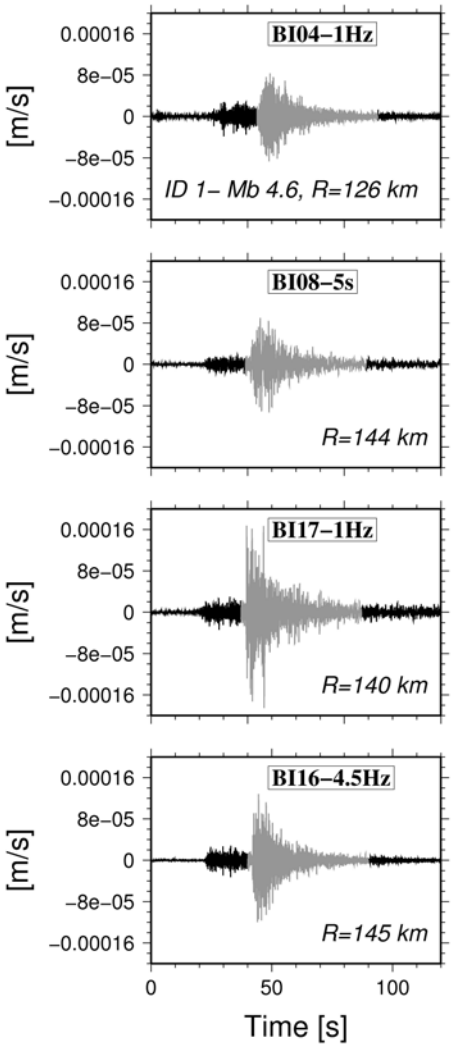

Figure 3: Recordings at four different stations of the 21.08.08 (mb = 4.6, ID = 1) earthquake (Table 1). The windows selected for the analysis are shown in gray. In each panel, the station ID (Figure 1), the epicentral distance R and the high pass corner frequency of the sensor are shown.

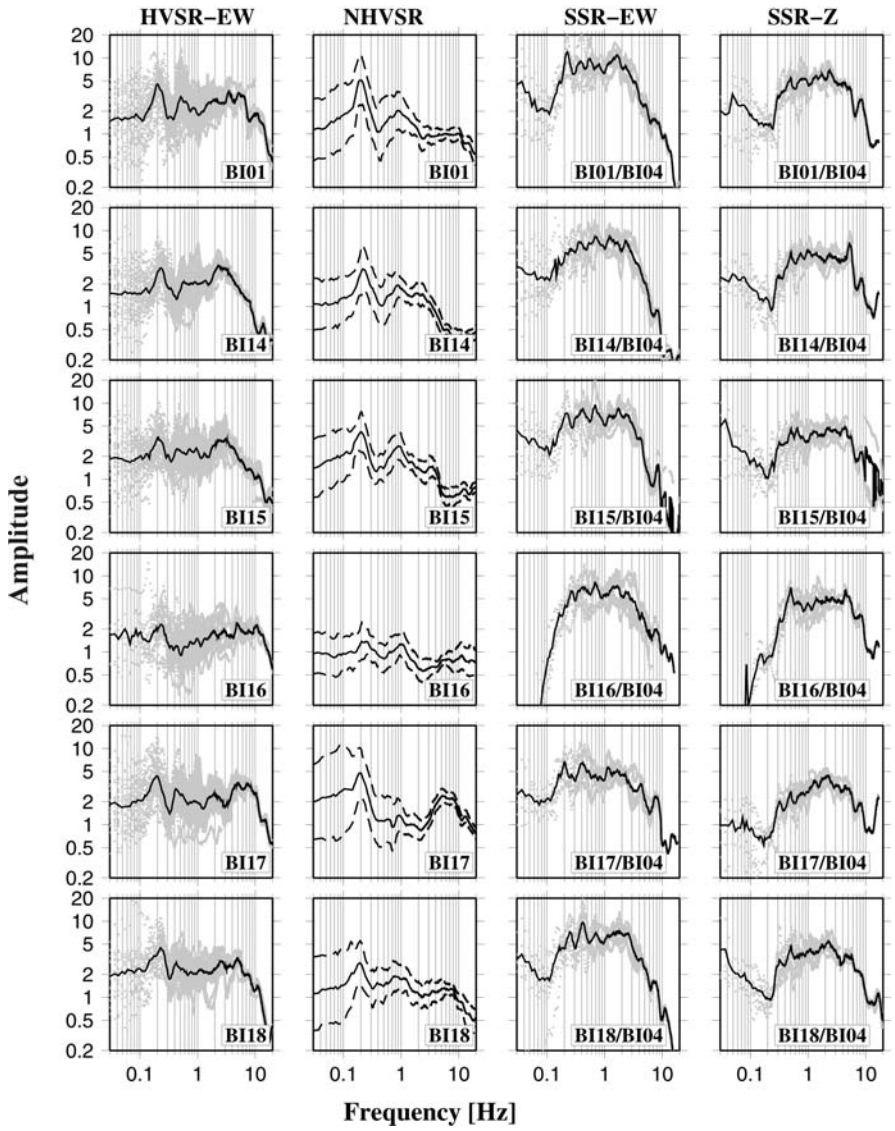

Figure 4: Different types of spectral ratios computed for the seismic stations installed in Bishkek. First column: Horizontal-to-Vertical spectral ratio (HVSR) for the S-wave windows selected over the East-West component; second column: Horizontal-to-Vertical spectral ratio of noise recordings (NHVSR); third column: Standard Spectral Ratios (SSRs) between the EW S-wave spectrum computed at each station and the correspondent spectrum at the reference station BI04; fourth column: the same as in the third column but for the vertical component. In the first, third, and fourth columns, the gray dots represent spectral ratios computed at frequencies where the signal to noise ratio is greater than 3, while the black curve

is the average ratio. In the second column, the mean ratio ± one standard deviation (dashed lines) is shown.

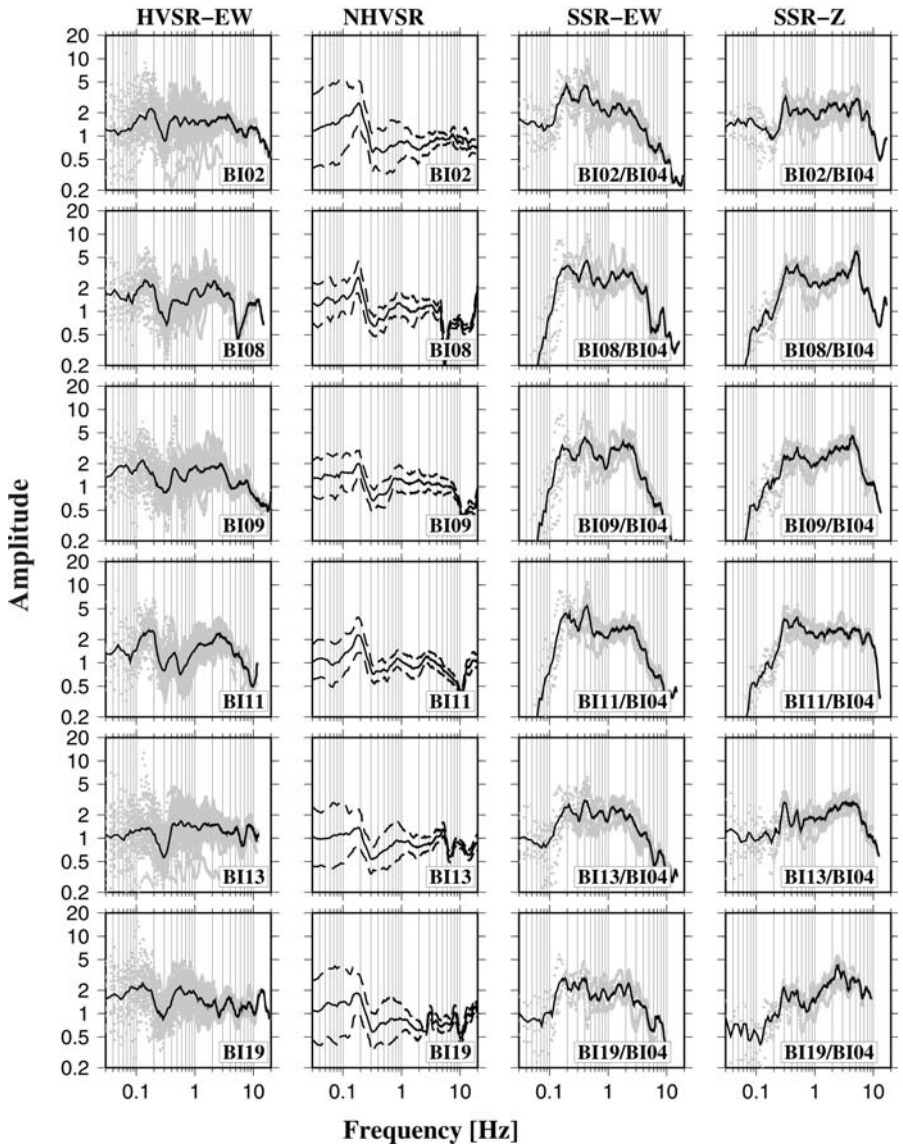

Figure 4: – Continue -

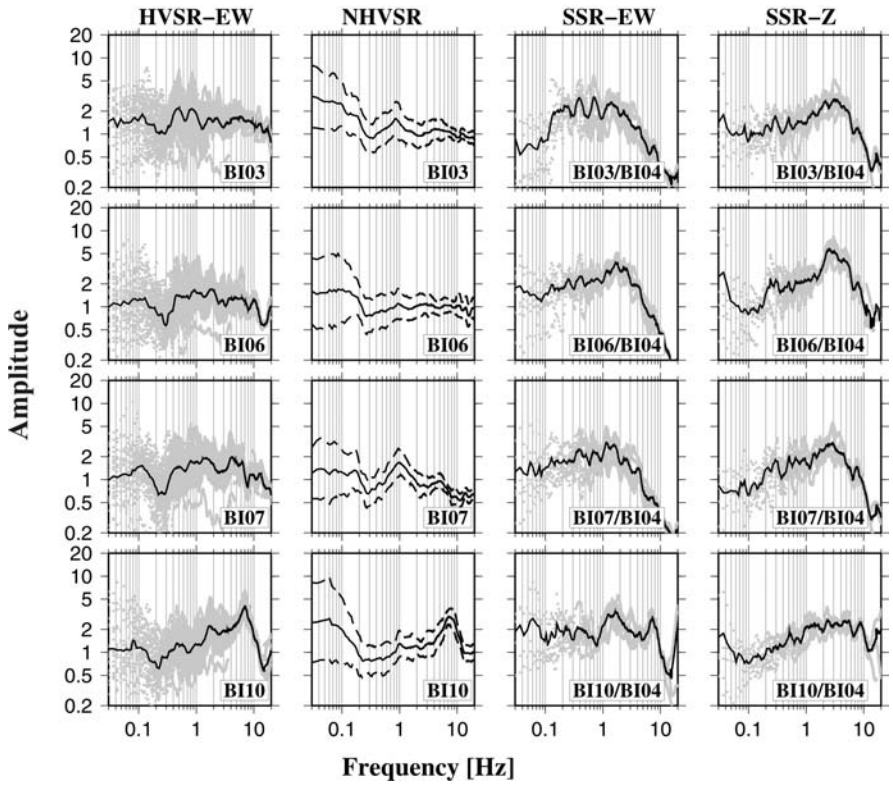

Figure 4: - continue –

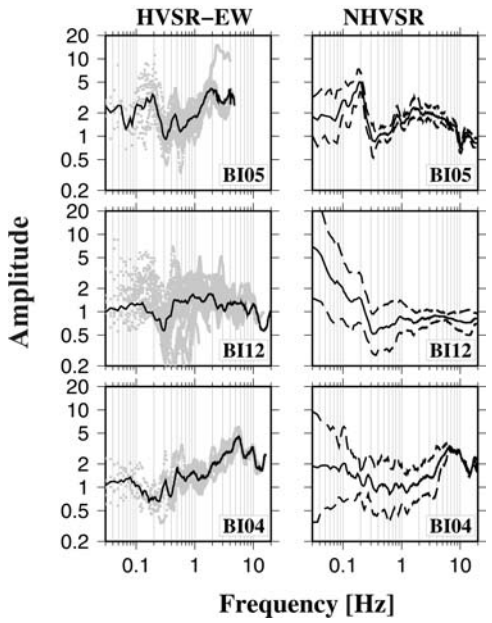

Figure 5: Horizontal to vertical spectral ratios for earthquake recordings (left) and noise (right), at 3 different stations of the temporary network (see caption of Figure 4 for explanations).

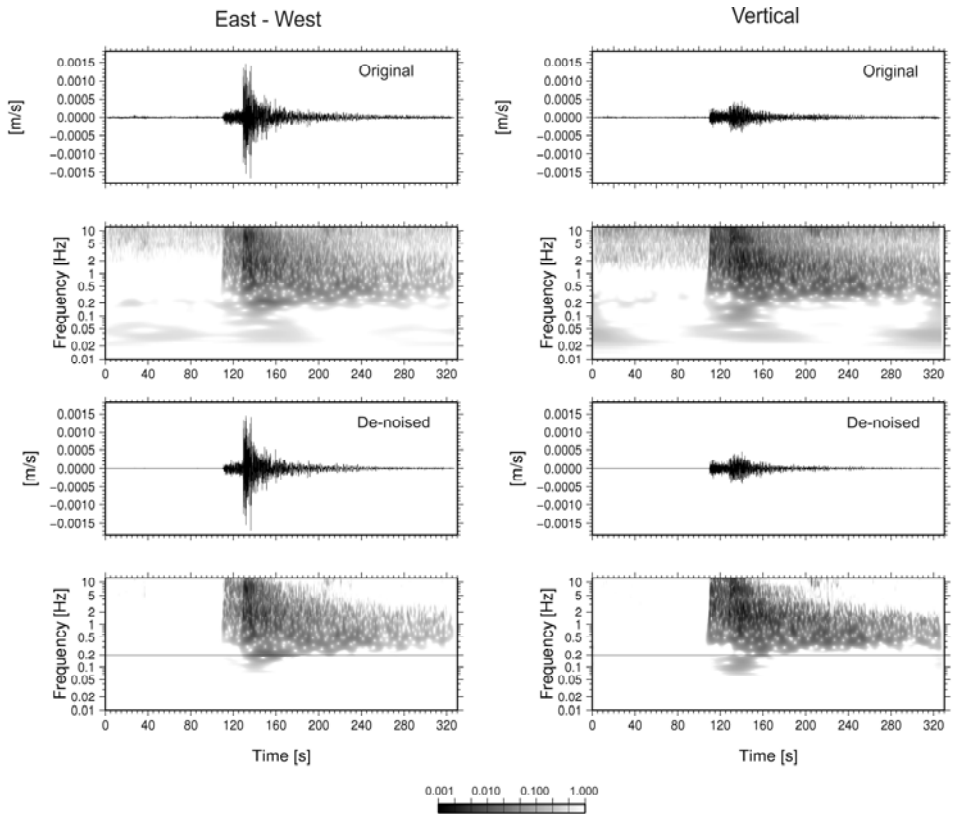

Figure 6: De-noising procedure applied in the time-frequency analysis, considering the east-west (left) and vertical (right) components. From top to bottom are shown the original recording of event 1 (Table 1) recorded at station BI17, the S-transform of the original recording, the de-noised recording and its S-transform. The color bar is for the S-transform results. See text for details about the procedure.

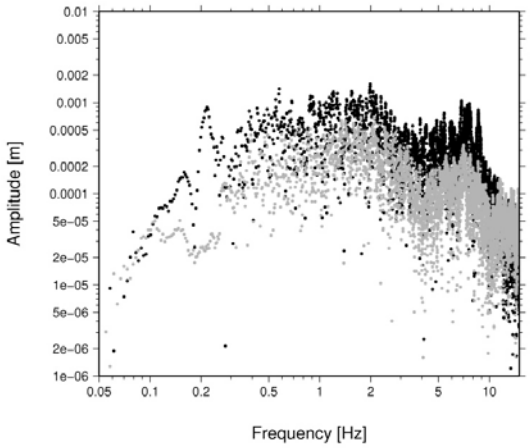

Figure 7: Fourier amplitude spectra of the de-noised seismograms shown in Figure 6. For each frequency, the black and gray dots represent the amplitude for the east-west (EW) and vertical (Z) components, respectively.

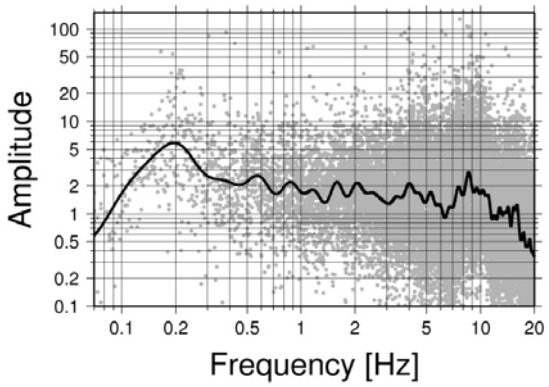

Figure 8: Horizontal (east-west) to vertical spectral ratios (gray circles at station BI17) obtained by considering de-noised seismograms from 4 different events (ID 1, 6, 15, and 36 in Table 1). The black line represents the trend observed in the data by performing a polynomial fit (Wessel and Smith, 1991).

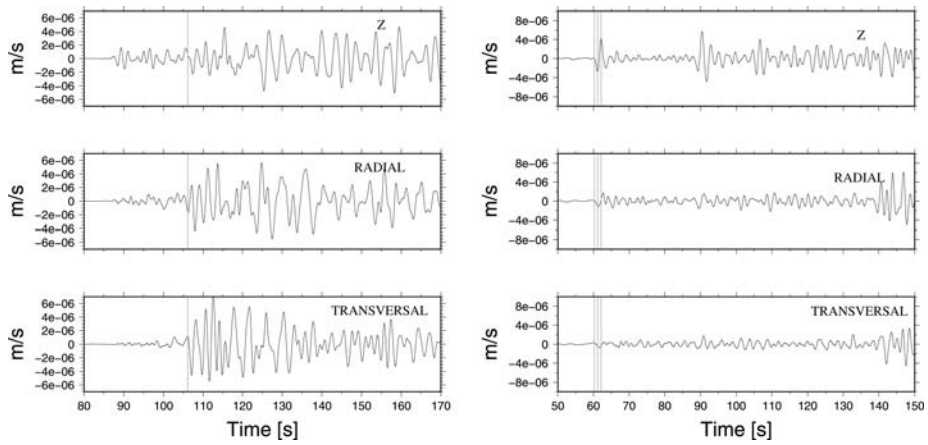

Figure 9: Vertical (top), radial (middle) and transversal (bottom) seismograms of events 1 (left) and 15 (right) of Table 1, recorded at station BI13. For event 15, only the first tens of seconds before the S-wave arrivals are shown. The time values on x-axis are referred to a generic reference time. Vertical gray lines indicate approximately the S-wave arrivals (left panels) and the arrival time of the first three peaks on the vertical component (right panels).

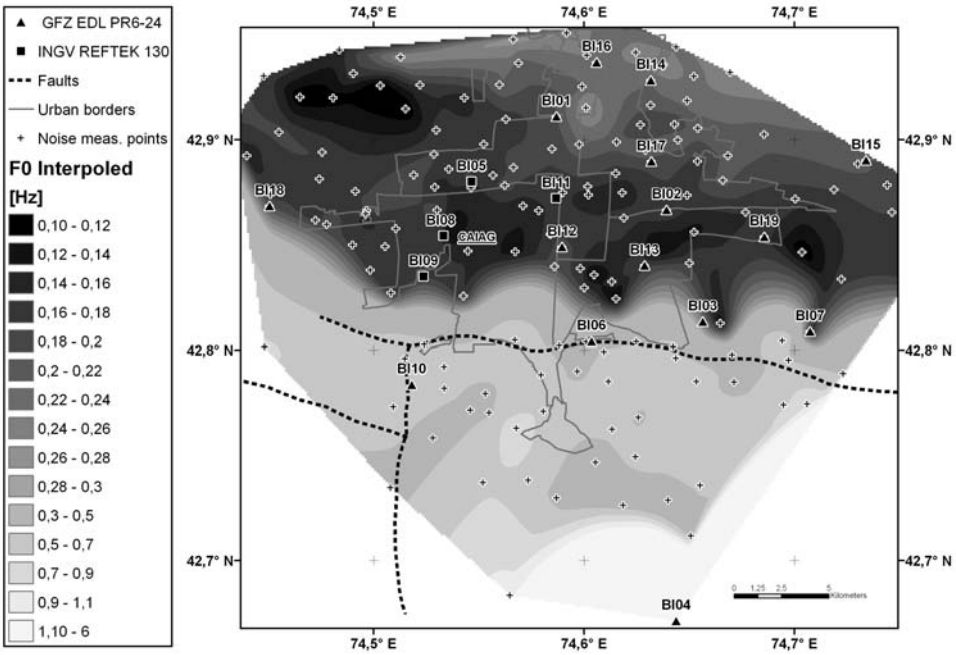

Figure 10: Map of the fundamental frequency of resonance estimated from noise measurements for the area around Bishkek (Kyrgyzstan).